Towards A Compact and Cost-effective Photoacoustic Sensing for Depicting Viscosity Information of Fluids

Abhijeet Gorey
Research and Innovation Labs
Tata Consultancy Services Ltd
abhijeet.gorey@tcs.com

Arijit Sinharay
Research and Innovation Labs
Tata Consultancy Services Ltd.
arijit.sinharay@tcs.com

Raj Rakshit
Research and Innovation Labs
Tata Consultancy Services Ltd.
raj.rakshit@tcs.com

Chirabrata Bhaumik
Research and Innovation Labs
Tata Consultancy Services Ltd.
c.bhaumik@tcs.com

Tapas Chakravarty
Research and Innovation Labs
Tata Consultancy Services Ltd.
tapas.chakravarty@tcs.com

Arpan Pal
Research and Innovation Labs
Tata Consultancy Services Ltd
arpan.pal@tcs.com

***Abstract*-In this study, we propose to use an intensity-modulated continuous-wave laser diode-based photoacoustic sensing technique to depict the change in viscosity of a sample. The proposed technique provides the compact, non-invasive, and cost-effective way to determine the change in viscosity. The efficacy of the technique to depict the change in viscosity of the sample is verified through experimentation. Here, five samples having different viscosities are prepared by mixing black ink dye and glycerol in different proportions. Experimentation is performed to obtain the continuous-wave photoacoustic (CW-PA) spectra from each of the samples and subsequently, few frequency domain features are evaluated as the potential marker for determining the change in viscosity of the sample. Also, a novel frequency-domain feature is identified to detect the change in viscosity of the sample. Results reveal that the proposed feature outperformed the conventionally used feature termed as Full Width at Half Maximum (FWHM) as the goodness of fit increases significantly to R^2 = 0.98 from R^2 = 0.91 (when used with FWHM only).**

Keywords: viscosity, Full Width at Half Maximum, CW photoacoustic sensing

I. INTRODUCTION

The characterization of mechanical properties of a sample is an emerging field of research in the medical and industrial domain [1]. Out of different mechanical properties (such as elasticity, density, etc.), viscosity is one of the critical thermosphysical properties of any material (primarily for liquids) [2]. The non-invasive identification of viscosity has found many applications in the clinical diagnosis and processing of composite materials.

In clinical science, the change in blood viscosity may be used as a diagnostic tool, as it is directly related to the blood flow [3]. Some studies have reported that monitoring the change in blood's viscosity can lead to the diagnosis of several hematological disorders, vascular changes, blood clots, etc. Also, continuous monitoring of blood's viscosity can be helpful to monitor the pathological variation in vessels and several other aetiological factors which may be associated with poor circulation [4-5]. Apart from clinical applications, monitoring of viscosity changes is extremely important in several industrial processes such as quality inspection of oil, paints, etc., and most importantly in the curing process of composite materials [6-8].

In addition to the above scenarios, a quick and cost-effective way of depicting a change in viscosity is a critical need for food processing industries also, wherein the knowledge of the change in viscosity information can lead to the measurement of dietary fibers, glucose tolerance, etc. [9-10]. Hence, the importance of determining the change in viscosity can be well understood from the above discussion. Although there are various methods and markers which are used to determine the change in viscosity of the sample, these methods are usually very laborious (i.e. taking the sample for chemical analysis, etc.), time-consuming and involve several complex calculations [11]. In the recent past, one of the highly sensitive and non-invasive sensing methods known as the photoacoustic (PA) sensing technique was applied to determine the change in viscosity of the liquid samples for quicker evaluation. Literature reveals that

results obtained through the PA sensing are in a close match with the theoretical calculations [12]. This proves the efficacy of the PA sensing method to determine the viscosity or change in viscosity of a sample.

In principle, PA sensing conventionally involves nano-second laser pulses of a specific wavelength to irradiate the sample. The sample upon absorption of these laser pulses undergoes thermionic expansion. While relaxing back, the sample releases the gained energy, in a non-radiative manner leading to the generation of pressure waves or acoustic waves. These time-domain acoustic waves are acquired by the ultrasound sensor placed near the sample. The acoustic wave from the ultrasound sensor appears to be the "N-shaped signal in time domain". Further, this time-domain acoustic signal is digitized and processed to extract the intended information [13-14]. The conventional pulsed laser based PA has found many applications, including the determination of change in viscosity of a liquid sample. However, the bulky and costly instrumentation involved with this method (i.e, with pulsed laser system) makes it ineffective for field deployment[15].

In this work, we explored the intensity-modulated continuous-wave (CW) laser diode-based PA sensing to detect the change in viscosity of the samples. The use of CW laser diode reduces the complexity of the overall system thereby making the technique compact, portable, and cost-effective. Although, intensity-modulated CW laser diode-based PA sensing has been explored for various biomedical applications (i.e. probing tissue samples)[16], to the best of our knowledge it has not been applied for depicting the change in viscosity in liquids. Thus, the focus of this work is to exploit continuous-wave laser diode-based PA measurement for monitoring the change in the sample's viscosity.

The paper is organized as follows: The working principle is presented in section II followed by detail experimental steps in section III. Next, experimental results were shown and discussed in Section IV in detail. Finally, the article is concluded along with a future scope of work in the Conclusion section.

II. WORKING PRINCIPLE

Traditionally, for determining the change in viscosity of the sample with PA sensing, the photoacoustic (PA) spectra are utilized. Literature reveals that viscosity can be determined by certain frequency domain features obtained through the PA spectra. Briefly, viscosity provides the damping force to the sample such that the higher is the viscosity, the lower is the damping force. Since the damping force is a measure of the reduction in energy (amplitude) of the oscillatory or vibratory motion, it typically affects the Quality factor (Q-factor) of the system [17-18].

Moreover, in a low Q-factor system the amplitude decays at a higher rate from its initial value, while the higher damping force represents the lower Q-factor. Equation (1) shows that, for the constant (or proximally shifted) centre frequency, the bandwidth of the signal is inversely proportional to the Q-factor, and therefore, the above discussion suggests that with the increase in viscosity of the sample, the bandwidth of the PA spectra reduces [19].

$$bandwidth = \frac{centre\ frequency}{Q-factor} \quad (1)$$

Mathematically, the bandwidth (ω) of a PA spectra in terms of coefficient of viscosity is given by (2),

$$\omega = a\ \sqrt{c_s^2 - \left(\frac{a\mu}{2\rho}\right)^2} \quad (2)$$

where, ω is the bandwidth of the PA spectra, *'a'* is the propagation phase constant, c_s is the speed of sound in the given medium, ρ is the density and μ is the coefficient of viscosity. Thus, (2) reveals that the increase in viscosity reduces the bandwidth. Furthermore, FWHM is proportional to (ω) as indicated in (3).

$$FWHM \propto \omega \quad (3)$$

Therefore, determining the FWHM of the PA spectra is commonly used to detect the change in bandwidth to monitor change in viscosity of the sample.

In conventional pulsed laser based PA, the FFT algorithm is applied to the time-domain PA signal to obtain the PA spectra. However, in this study PA spectra is formed directly in frequency domain by irradiating the sample with known frequencies and recording the corresponding responses. More specifically, the intensity of a continuous wave laser diode is sinusoidally modulated for 5 cycles at a specific frequency to form a laser burst. This modulated laser wave burst is irradiated to the sample and the resulting sinusoidal acoustic pressure variation is acquired by the ultrasound sensor. Then the signal is digitized and stored in the computer for further processing.

The resulting pressure signal is supposed to be of the same frequency and burst duration as that of the corresponding excitation. The experiments are repeated for different excitation frequencies (i.e. starting with some minimum excitation frequency f_{min} and stopping at some maximum excitation frequency f_{max}) and the corresponding peak-peak amplitude (Vpp) of the resulting acoustic pressure signal is noted for each of the frequencies. A plot of Vpp vs different excitation frequencies (f) produces the required CW-laser diode based photoacoustic (CW-PA) frequency spectra from which FWHM is calculated to infer the change in viscosity. This is to note that the CW-PA spectra are Gaussian fitted using (4),

$$y_n = h.exp^{\left(-\left(\frac{x_n - m}{\sigma}\right)^2\right)} \quad (4)$$

where, y_n = predicted value, h = peak height above the base line, x_n = value of independent variable, m = position of the maximum, σ = standard deviation. In our case, y_n represents the peak-peak amplitude values (*Vpp*) and x_n represents frequency values *(f)*. Further, the Gaussian is normalized to unity (i.e. h =1) to avoid issues due to possible change in absorption properties of the sample.

FWHM is calculated from the obtained normalized Gaussian fitted CW-PA spectra by using the well-known equation stated below:

$$FWHM = 1.66 * \sigma \quad (5)$$

where σ is the standard deviation of the Gaussian fit.

Subsequently, a new feature, *F1*, is identified wherein the FWHM is combined with the spectral area through (6),

$$F1 = \frac{FWHM}{Spectral\ Area} \quad (6)$$

where 'Spectral Area' corresponds to the area under the fitted Gaussian curve. Further, both features (FWHM and F1) are evaluated based on the co-relation (goodness of fit) values (i.e. R^2). More details about exact experimentation steps are described in the next section.

A pictorial view of a typical CW-PA spectra (Vpp vs f) is shown in Fig. 1 where data points, fitted curve, FWHM and area under the curveare marked for clarification purpose(qualitative representation) only.

III. EXPERIMENTAL SETUP

This section talks about the experimental setup and procedures in details. First, we talk about the instrumentation and next we talk about the sample preparation steps.

A. Instrumentation

Fig. 2 shows the schematic of the overall experimental set-up. The CW-PA technique mainly comprises excitation and acquisition systems. The excitation in the CW-PA technique is enabled by the intensity-modulated continuous-wave laser diode beam. The laser diode used here is L450P1600M from Thorlabs Inc. USA, having a center wavelength, 450nm, and maximum power of 1.6W. The laser diode is driven by an in-house-built laser driver.

The developed laser driver can deliver the maximum current of 1.2A at a modulation frequency of 3MHz (maximum). The modulation signal to the laser driver circuit is provided through the function generator. In our study, the laser diode beam is sinusoidally modulated through 5 cycles in the frequency range of 0.1-1.3 MHz at an interval of 20 kHz.

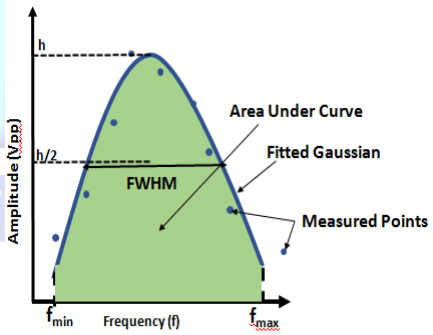

Fig 1: Pictorial representation of a CW-PA spectra

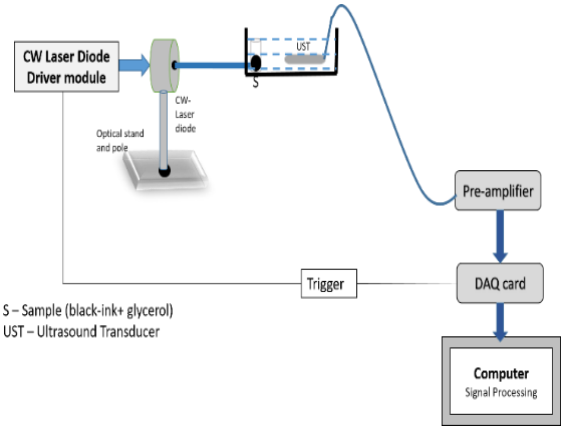

Fig 2: Schematic representation of experimental set-up used for CW-PA sensing

The ultrasound signal from the sample is acquired by the ultrasound sensor (from Olympus, V303-SU, center frequency at 0.81 MHz) and it is placed axially to the sample container as shown in Fig. 2. Further, a custom-built pre-amplifier board having a fixed gain of 60dB is used to amplify the acquired CW-PA signal. The amplified CW-PA signal is further averaged 128 times to improve its SNR. The signal is averaged in real-time in a Digital Storage Oscilloscope (DSO) running at a sampling rate of 200 MSPS. The averaged signal is stored in the memory of DSO. Since, for a real-time averaging the excitation and acquisition system must be synchronized, the excitation and acquisition system are triggered through the 1kHz, 3V (TTL) signal.

Subsequently, this CW-PA signal data (stored in DSO memory) is transferred to the computer for further signal processing using MATLAB. The peak-peak voltage of the CW-PA signal is determined at all measured frequencies and further this peak-peak voltage is plotted against its corresponding frequencies to get the desired CW-PA spectra. To extract the viscosity information from the sample, the obtained CW-PA spectra are Gaussian fitted, normalized to their peak amplitude, and then FWHM is determined. The spectra are normalized to remove any issues due to the absorption property of the sample.

During the complete set of experimentation power modulation of the laser diode is kept constant i.e. 500mW peak-peak, at all frequencies, with a beam diameter of 5mm at a sample plane. Moreover, the sample container and the ultrasound sensor are immersed in the glass container filled with water to have better acoustic coupling.

B. Sample Preparation

For experiments, five samples of the glycerol-black-ink mixture are prepared by keeping the concentration of black-ink to be fixed and varying the concentration of glycerol from 0 to 100 % in the steps of 25 % as shown in Table I. The glycerol was added to the ink solution, stirred well, and kept for 10 minutes for obtaining consistency in the sample. These five sets of samples act as varying viscous model fluids for our experimentation. Literature reveals that the addition of glycerol to the black ink dye change its viscosity. Moreover, the percentage change in viscosity is proportionate to the volume of glycerol added to the sample. Hence, while preparing the samples using black ink dye and glycerol, the volume of glycerol is added in a definite proportion to change its viscosity. Further, these samples are experimented to obtain there CW-PA spectra and frequency domain features are calculated. The shift in these frequency domain features is observed with the change in viscosity of the sample. The entire set of experiments are executed at a constant temperature of approximately 22 ^{o}C. For each sample, the experiments are repeated three times and hence the reproducibility of the result is verified.

IV. RESULTS AND DISCUSSION

Fig. 3 shows a typical CW-PA signal for one of the black ink-glycerol samples at an excitation frequency of 0.7 MHz, wherein the peak-peak voltage (Vpp) is shown. The acquired signal exactly matched with the frequency and burst duration of the excitation signal as expected. Similarly, for the same sample (V5 as per Table I), the excitation frequency was varied from 0.1-1.3 MHz in the steps of 20 kHz and the CW-PA spectra are obtained and Gaussian fit is applied. FWHM is obtained from the fitted curve as shown in Fig. 4.

TABLE I: CHANGE IN GLYCEROL CONCENTRATION TO PRODUCE DIFFERENT VISCOSITY SAMPLES

Sample No.	Black ink (ml)	Glycerol (ml)
V1	2	0
V2	2	0.5
V3	2	1
V4	2	1.5
V5	2	2

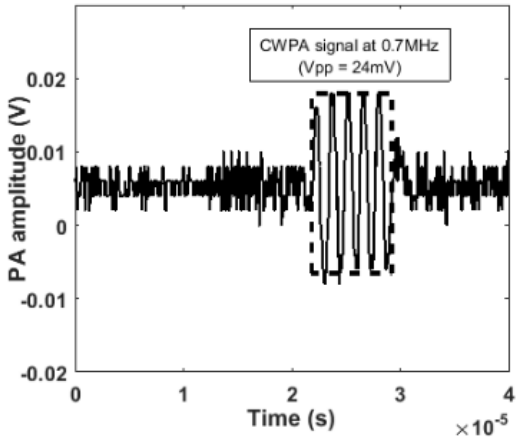

Fig 3: CW-PA signal at 0.7 MHz

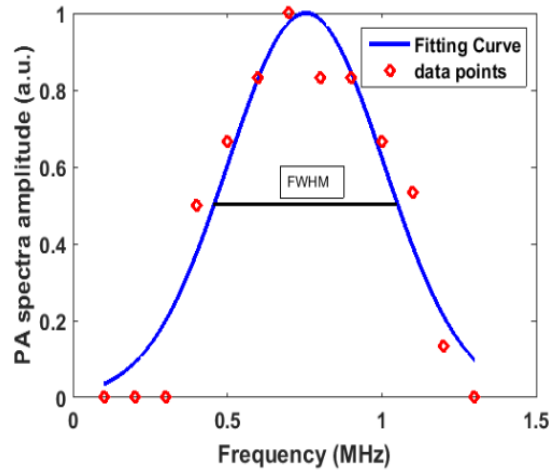

Fig 4. Normalized CW-PA spectra of a sample (V5)

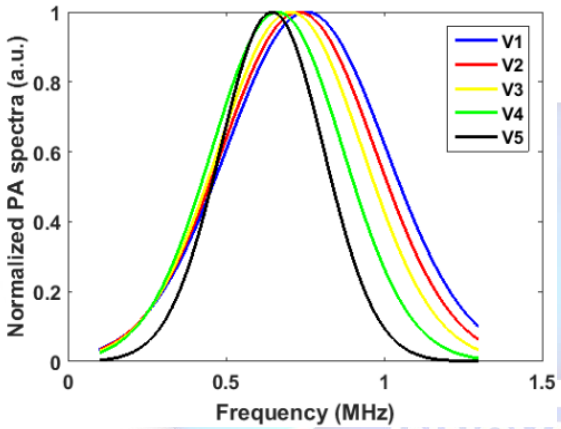

Fig 5: CW-PA spectra for different viscosity samples

Similar plots were obtained from all the samples (V1-V5) and co-plotted in Fig 5. With the increase in viscosity from V1 to V5, the shift in resonance spectra, as well as the shrinking of resonance width, is seen in Fig. 5. For example, FWHM for V1 is found to be 0.75 MHz whereas FWHM for V2 is found to be 0.72 MHz.

Fig. 6 depicts the change in FWHM for the change in viscosity of the samples. The fitted (linear fit) plot reflects that the FWHM reduces almost linearly with the increase in viscosity as supported by (2) and (3). The R^2 value of the fitted line turns out to be 0.91 indicating that FWHM can be a potential marker for tracking change in viscosity.

However, for very small change in viscosity, it may become difficult to use FWHM as a reliable marker as R^2 value is still little far from 1.0.

Therefore, a new feature F1 is identified which reveals substantial improvement in R^2 as shown in Fig 7. Here, the R^2 value is increased to 0.98 showing a stronger relationship between F1 and change in viscosity than that of FWHM and change in viscosity. The reason for increase in the value of R^2 is due to use of spectral area information along with the FWHM. As the value of FWHM changes with the change in viscosity, its spectral area also changes. Thus, fusion of two individual features (i.e. FWHM and 'spectral area') produced superior results.

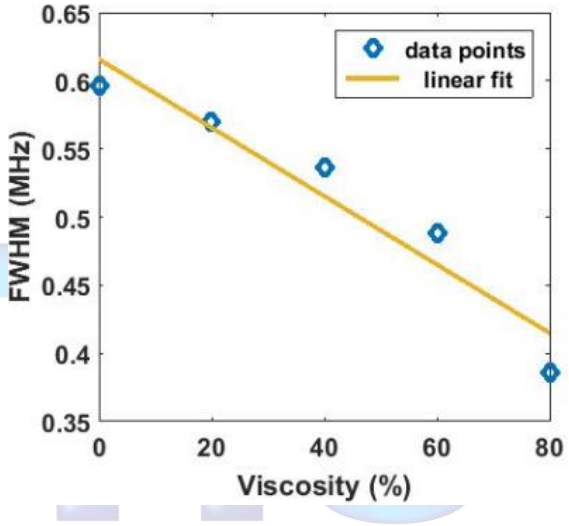

Fig 6: FWHM Vs viscosity of the sample

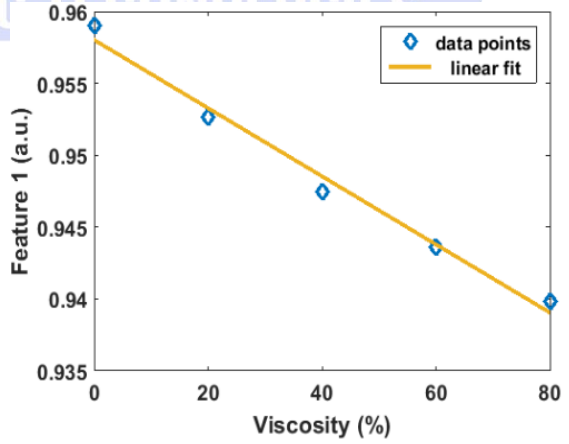

Fig 7: Change in (F1) with respect to change in viscosity

CONCLUSION

In this study, the efficacy of laser-diode based CW-PA sensing is explored for tracking change in

viscosity of fluids. The experimental results justify our approach towards compact and portable PA sensing for depicting the change in viscosity of fluids. Further, the proposed frequency-domain feature outperforms the conventional FWHM feature as the goodness of fit parameter (R^2) increased from 0.91 to 0.98. Thus, this finding supports the possibility of building a compact, portable and affordable PA sensing system for a range of industrial applications. In our future attempt, we plan to apply our approach to actual industrial fluids.

REFERENCES

1. Dave VS, Shahin HI, Youngren-Ortiz SR, Chougule MB, Haware RV. Emerging technologies for the non-invasive characterization of physical-mechanical properties of tablets. International Journal of Pharmaceutics. 2017 Oct 30;532(1):299-312.
2. Y. Z. Wang, X. M. Xiong, and J. X. Zhang, J. Rheol. 52, 999–1011 (2008).
3. F. Gao, X. Feng, Y. Zheng, and C. D. Ohl, J. Biomed. Opt. 19, 067006 (2014).
4. Sakai H, Takeoka S, Park SI, Kose T, Nishide H, Izumi Y, Yoshizu A, Kobayashi K, Tsuchida E. Surface modification of hemoglobin vesicles with poly (ethylene glycol) and effects on aggregation, viscosity, and blood flow during 90 exchange transfusion in anesthetized rats. Bioconjugate chemistry. 1997 Jan 29;8(1):23-30.
5. Whittaker SR, Winton FR. The apparent viscosity of blood flowing in the isolated hindlimb of the dog, and its variation with corpuscular concentration. The Journal of physiology. 1933 Jul 10;78(4):339.
6. Kim JS. On-line cure monitoring and viscosity measurement of carbon fiber epoxy composite materials. Journal of Materials Processing Technology. 1993 Feb 1;37(1-4):405-16.
7. Ayub KV, Santos Jr GC, Rizkalla AS, Bohay R, Pegoraro LF, Rubo JH, Santos MJ. Effect of preheating on microhardness and viscosity of 4 resin composites. J Can Dent Assoc. 2014 Jan 1;80(12):e12.
8. Chen JY, Hoa SV, Jen CK, Wang H. Fiber-optic and ultrasonic measurements for in-situ cure monitoring of graphite/epoxy composites. Journal of composite materials. 1999 Oct;33(20):1860-81.
9. Roberts SS, Davidson R. Cure and fabrication monitoring of composite materials with fibre-optic sensors. Composites science and technology. 1993 Jan 1;49(3):265-76.
10. Jenkins DJ, Wolever TM, Leeds AR, Gassull MA, Haisman P, Dilawari J, Goff DV, Metz GL, Alberti KG. Dietary fibres, fibre analogues, and glucose tolerance: importance of viscosity. Br Med J. 1978 May 27;1(6124):1392-4.
11. M. Papi, G. Maulucci, G. Arcovito, P. Paoletti, M. Vassalli, and M. De Spirito, Appl. Phys. Lett. 93, 124102 (2008).
12. Lou C, Xing D. Photoacoustic measurement of liquid viscosity. Applied Physics Letters. 2010 May 24;96(21):211102.
13. Li C, Wang LV. Photoacoustic tomography and sensing in biomedicine. Physics in Medicine & Biology. 2009 Sep 1;54(19):R59.
14. Duan T, Lan H, Zhong H, Zhou M, Zhang R, Gao F. Hybrid multi-wavelength nonlinear photoacoustic sensing and imaging. Optics letters. 2018 Nov 15;43(22):5611-4.
15. Gorey A, Jacob PM, Abraham DT, John R, Manipadam MT, Ansari MS, Chen GC, Vasudevan S. Differentiation of malignant from benign thyroid nodules using photoacoustic spectral response: a preclinical study. Biomedical Physics & Engineering Express. 2019 Mar 28;5(3):035017.
16. Gorey A, Biswas D, Kumari A, Gupta S, Sharma N, Chen GC, Vasudevan S. Application of continuous-wave photoacoustic sensing to red blood cell morphology. Lasers in medical science. 2019 Apr 4;34(3):487-94.
17. Morgan GW, Kiely JP. Wave propagation in a viscous liquid contained in a flexible tube. The Journal of the Acoustical Society of America. 1954 May;26(3):323-8.
18. Yuya PA, Hurley DC, Turner JA. Relationship between Q-factor and sample damping for contact resonance atomic force microscope measurement of viscoelastic properties. Journal of Applied Physics. 2011 Jun 1;109(11):113528.
19. Zhao Y, Yang S, Wang Y, Yuan Z, Qu J, Liu L. In vivo blood viscosity characterization based on frequency-resolved photoacoustic measurement. Applied Physics Letters. 2018 Oct 1;113(14):143703.